# Stand-Alone Hemisphere-Tank Rupture in Tunnel Fire: Effect of Hydrogen Inventory on Blast Wave Strength in Far Field

**Shentsov V.*, Makarov D., Dery W.**

*Hydrogen Safety Engineering and Research Centre (HySAFER),*
*Ulster University, Shore Road, Newtownabbey, BT37 0QB, UK*
**Corresponding author's email: v.shentsov@ulster.ac.uk*

## ABSTRACT

High-pressure hydrogen onboard storage rupture in a fire generates blast wave and fireball. These hazards are not yet investigated enough, especially in a tunnel. Consequences of such event, e.g. a blast wave, could be devastating depending on amount of stored hydrogen and tunnel dimensions. This raises the question about the dependence of blast wave overpressure on hydrogen inventory in the tank. The problem is studied here numerically. Large eddy simulation (LES) turbulence model with the eddy dissipation concept (EDC) for combustion were employed in series of numerical simulations in three different tunnel cross-sections with four hemispherical tank volumes at pressures of 94.5 MPa. The dependence of blast wave overpressure on hydrogen inventory is defined. The results are conservative and require experimental validation in tunnel tests.

**KEYWORDS:** Tunnel, blast wave, tank rupture, inventory.

## INTRODUCTION

As the worlds demand for global energy increases for each day, uncertainty regarding fossil and hydrocarbon energy supply sources and long-term effects on the environment are of major concern. An industry-led effort in aims to steer away from fossil-fuelled energy carrier dependencies are therefore gaining vast interest. A growing attitude towards a more environmentally friendly and sustainable energy, hydrogen is specifically targeted in the energy evolution with it representing a clean fuel with high energy content. Presently, utilisation of hydrogen as a commercial energy carrier is being veered onto private and public automotive domains, such as in the transportation sector (e.g. cars and buses). Major car companies such as Honda, Mercedes Benz, Hyundai and Toyota etc. all have cars available for the public in select markets, with hydrogen stations growing steadily (additional 15 000 new hydrogen filling stations are slated for year 2030 globally) [1].

Even though tunnels are an obligated part of everyday vehicular transportation, there are a number of safety concerns not extensively researched upon. The potential hazards associated with hydrogen vehicles in road tunnels was internally identified and investigated by a project called HyTunnel [2]. Mainly non-instantaneous hydrogen releases (i.e. through vents) were illustrated through reviewing current hydrogen designs, tunnel design practice and a programme of experiments and computational fluid dynamics (CFD) modelling performed for selected scenarios. Despite specifying a simultaneous release of a large mass of hydrogen found to be more hazardous compared to when the same mass being released through a single vent, a study extended to examine this issue was left unattended. One of the main knowledge gaps is of a blast wave that can be generated by catastrophic onboard tank rupture in a tunnel caused by fire. The regulation requires that each onboard storage tank is equipped by thermally-activated pressure relief device (TPRD) to

Proceedings of the Ninth International Seminar on Fire and Explosion Hazards (ISFEH9), pp. 1314-1323
Edited by Snegirev A., Liu N.A., Tamanini F., Bradley D., Molkov V., and Chaumeix N.
Published by Saint-Petersburg Polytechnic University Press
ISBN: 978-5-7422-6498-9 DOI: 10.18720/spbpu/2/k19-72

prevent tank rupture in a fire by releasing stored hydrogen. However, a TPRD can fail to function, be blocked from a fire during accident, or be not affected in case of localised fire [3].

Tunnels represents a structure strong enough to withstand tremendous pressure from all sides, as the close-in and reflection effects of the tunnel distinguishes characteristics known from an unconfined space [4]. It was found that the blast wave generated in a tunnel will propagate along the tunnel practically without decay independent of the tunnel length [5]. This could have serious safety implications. A significant incident involving a hydrogen project could negatively impact the public's perception and clean alternatives to conventional energy systems may never experience commercial deployment successfully [6]. This involves covering different aspects of vehicle conduct within day-to-day activities, anticipating accidents and accounting for unforeseen consequences. This information is of primary interest for public and especially for first responders.

There is a paucity of data in experimental work conducted in tunnels of natural provenance and original size involving pressurised tank bursts. Of those available, experimental and numerical studies have been performed to understand the phenomena and develop engineering tools for blast wave propagation in confined spaces (i.e. garages and tunnels) using explosive charges such as TNT [7], [8], [9]. Early understanding of a blast wave from a high explosive source within a structure was claimed to undergo reflections with the inner surface, with decay after each reflection, "eventually, the pressure settles to a slowly decaying level, which is a function of the volume and vent area of the structure and the nature and energy release of the explosion" [10].

Experiments in full-scale tunnels are unaffordably too expensive. The use of CFD eliminates this restriction and allows the ability to use realistic scenarios. Following experimental studies by Zalosh and Weyandt [11], Kim et al. [12] simulated the blast wave and fireball in their test numerically. The realizable $k$-$\varepsilon$ turbulence model was applied and combustion was simulated by the eddy dissipation model, which reproduced the experimental trends. Weyandt [13] performed a bonfire test with Type 4 tank of 72.4 L volume and storage pressure of 34.3 MPa without TPRD to estimate the blast wave and fireball parameters. In 2015, an original theoretical model was developed that allows to calculate parameters of a blast wave from a tank rupture in a fire at different distances in the open atmosphere [14]. In this paper, it was concluded that about 5% of chemical energy of released hydrogen contributes to the blast wave strength through its combustion for a stand-alone tank, and 9% of chemical energy for an under-vehicle tank. In addition, the harm to people and damage to buildings from a blast wave was used to assess hazard distances.

This overall research seeks the ability to explore, pin down and mitigate hazards associated with the current understanding of onboard hydrogen storage applications. With a non-zero probability of a high-pressure hydrogen storage tank rupturing catastrophically, this phenomenon is pivotal to have gained a complete overview over, prior to an incident and its aftermath. The hazards following such an event are found significant, not only in the near vicinity of the blast source, but also in the far field for both humans and structures. Methods of predicting effects of the blast wave and fireball from a pressurised vessel is found in the literature not straightforward – especially the former catering for intricate rupture dynamics and volumetric effects of various tank sizes.

Our previous study of tank rupture inside the tunnel [15] was based on the conservative scenario of a road tunnel with smallest cross-section area and a storage tank with the highest amount of hydrogen for passenger cars (70 MPa, 140 L). The established quasi-steady blast wave in the tunnel was 25 kPa for the case of rupture without combustion (observed at 40 m from the tank location) and 37 kPa for the tank rupture with combustion (blast wave stabilised at 30 m), i.e. 50% higher for a tunnel scenario. This result confirmed our previous conclusion that hydrogen combustion at the contact surface between air and hydrogen behind the shock increases the blast wave strength. Both values of blast wave overpressure are above of the serious injury threshold of 16.5 kPa [16].

The previous RANS model has been changed in this study to more advanced LES for turbulence, and the EDC for combustion. In addition, the further increase of pressure and temperature in the tank before rupture observed has been taken into account in these simulations, measured in experiments [17]. Two fire tests were carried with both tanks pressurised up to 70 MPa. Test 1 was conducted with Type 4 tank of 35 L volume in which the pressure at the moment of rupture was 94.54 MPa, i.e. 35% higher than nominal working pressure. In Test 2, a Type 3 tank of 36 L volume was used, the pressure before burst increasing to 99.47 MPa, i.e. 42% higher than before the test.

## NUMERICAL MODEL

Simulations are performed using ANSYS Fluent. The pressure-based solver coupled with PISO pressure-velocity algorithm is applied. The numerical model used in this study included the use of LES for turbulence with the Smagorinsky-Lilly model for simulation of sub-grid scale turbulence and the EDC combustion employing one-step reaction. The comparison with 37 reactions scheme did not show any difference in pressure but provided essential speedup in calculation. The governing equations are based on the filtered conservation equations for mass, momentum, and energy in their compressible form. The tunnel walls and floor are specified as non-adiabatic to allow heat transfer from the combustion no-slip wall conditions applied. The external non-reflecting boundary is defined as pressure outlet with zero-gauge pressure. The second order upwind discretization scheme is used for pressure to improve simulation accuracy for compressible flows, the second order upwind scheme is used for convective terms. The first order is employed for time advancement. To conserve the mechanical energy of compressed hydrogen the tank volume with "ideal gas" in simulations was reduced compared to real tank volume (the pressure was kept as in experiment to get the same starting shock pressure) using the following equation $V_{ideal} = V_{real} - mb$. Were $V$ is volume ($m^3$), $m$ is mass (kg) and $b = 7.69 \cdot 10^{-3}$ is the co-volume constant ($m^3$/kg). The original time step adapting technique was employed to maintain a constant Courant-Friedrichs-Lewy (CFL) number at value of 0.2 in all simulations based on sensitivity study. All calculations are carried out with 20 iterations per time step.

## MODEL VALIDATION

This model has been validated against experiments with stand-alone tank rupture in fire in the open atmosphere at storage pressures of 35 MPa [13] and 70 MPa [17]. Good agreement between the simulations and experimental data for the blast wave and fireball dynamics has been achieved (see Fig. 1 for the 35 MPa test) [10]. Figure 1 shows the comparison of experimental (solid) and simulated (dashed) pressure transients at three different locations. The model reproduces the experimental maximum peaks and dynamics results very well. The first peak at distance 1.9 m from the tank (achieved at 1.4 ms) is overestimated in simulations by approximately 50 kPa. This is thought due to neglecting the energy loss to propel tank fragments, destroy the burner structure and to crater the ground.

Figure 2 shows the comparison of fireball size in the test and simulations at 45 ms after the tank rupture. Both the size and the shape of fireball, including the area of bridging shock, are well reproduced. The validated model in the open space model for stand-alone tank is then applied for a series of simulations inside the tunnel to first and foremost assess the effect of inventory on the blast strength.

## TUNNEL GEOMETRY

For determination of the tunnel geometry, the minimum standard solution for cross-section areas in road tunnel following the guidelines for the equipment and operation, with regards to road design

and alignment was considered. Without requirements accommodating passage for an eventual broken-down vehicle, the width of the road necessary is standardised as 3.5 m including a verge area of a meter added on each side referring to the area outside the marked driving lane [18]. These minimum cross-sectional dimensions for the lane width of the tunnel were kept unaltered for all three tunnels considered in this study. The chosen number of lanes (1, 2 and 5) for each tunnel were due to several reasons. The first tunnel chosen, a single lane with cross-section area of 24.1 $m^2$ enclosure mostly found on country roads, was considered to treat the worst-case scenario; the blast wave would expand and dissipate less through the close-in effects of the tunnel wall. The second tunnel encapsulating the other end of the worst-case scenario scale accommodating the largest cross-sectional area currently built, the Yerba Buena tunnel as part of the San Francisco–Oakland Bay Bridge [19]. It features a double-decked design each with five lanes, and the larger upper deck with a total cross-section area of 139.1 $m^2$ was chosen for this study. Road traffic is mostly constructed using two lanes, and in some countries (e.g. Germany) constitute up until 90% of all rural roads including tunnels [20]. Therefore, the third tunnel used in this study contained two lanes as the median with cross-section area of 39.5 $m^2$. The one and two lane tunnels both has an inner tunnel height of 4.5 m, the minimum required headroom for road traffic [21]. The inner height of the five-lane tunnel was set at 7.2 m.

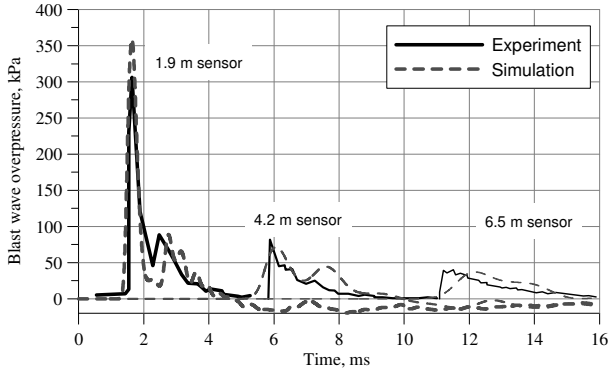


**Fig. 1.** Pressure dynamics experimental (solid) vs simulated (dashed).

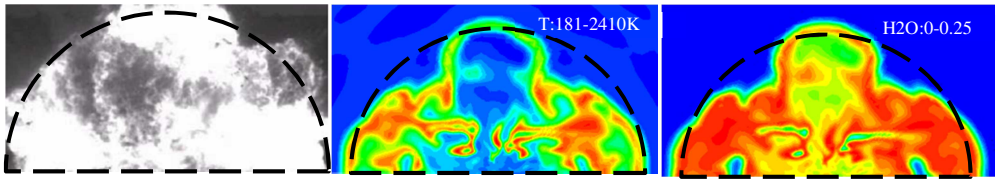


Fig. 2. Fireball size at 45 ms: experiment (left), simulated temperature (centre) and water mole fraction (right).

## COMPUTATIONAL DOMAIN

A total volume of the domain (*LxHxW* = 300x100x75 m) being 2.25E+06 $m^3$, a considerable size of domain was used to place the tunnel within, limiting the boundary conditions altering any pressure dynamics in and around the tunnel. Each tunnel employed was placed on the midpoint of the outer boundary domain, with a fixed length of 200 m. The rupture location of the high-pressure hydrogen enclosure was set 50 m from one exit, 150 m from the other exit. This was done mostly to ensure a stabilized and undisturbed pressure propagation and stabilisation throughout the long end of the tunnel without influence from the other exit. The control volumes (CV) of the boundary zone, outside the tunnel, were tetrahedral shaped and varied in size relative to its position away from the

tunnel. This was carried out with a scale factor of 2 and a max CV size of 10, allowing the actual maximum CV size used for meshing to get as big as 2x10=20 m in size. However, this would be dependent on the need of accuracy required in its position. CVs close to the tunnels exits would be smaller in size, set to be 0.1 m. One of the advantages using ANSYS Fluent is the ability to convert mesh, with one option being combining tetrahedral cells into polyhedral ones and executed for the boundary zone across all three tunnels. A summary of the tunnel dimensions and total number of CVs for each tunnel are listed in Table 1.

**Table 1. Tunnel dimensions and control volumes**

| Tunnel | Cross-section, $m^2$ | Control volumes |
|---|---|---|
| **Single lane** | 24.1 | 201 156 |
| **Double lane** | 39.5 | 175 596 |
| **Five lanes** | 139.1 | 450 226 |

CVs inside the tunnel domain were of hexahedral shape, enclosing not only the entire tunnel boundary, but also the high-pressure hydrogen tank area. A hexahedral mesh was used to ensure a better approximation of the initial high gradient pressure and velocity values. The mesh size ranged from 0.02-0.03 m from the hydrogen surface and using a BiGeometric meshing law, would grow ranging from 0.05 to 0.75 m uniformly. This refined area around each respective tank sizes were kept unchanged across all three tunnels for consistency and stability. The entire domain containing sub-zones of tunnel and tank geometry are illustrated in Fig. 3.

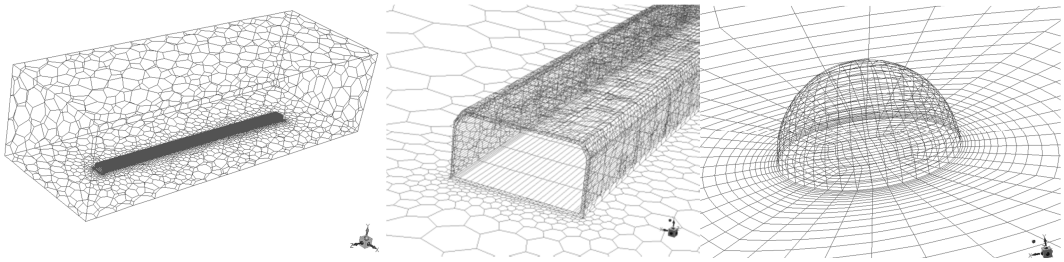

**Fig. 3.** Mesh of the entire domain (left), cut out of the tunnel exit (middle) and hydrogen hemispherical tank (right).

The quality of the mesh was measured and assured in Fluent by the maximum orthogonal quality and aspect ratio and the minimum orthogonal skewness. The quality ranges from 0 to 1, where values close to 0 correspond to low quality in the case of the minimum orthogonal quality and reversed for the case of the maximum orthogonal skewness. A value of 0.4 and 0.7 were obtained respectively for each ran case with a corresponding maximum aspect of 28.4. The bottleneck for improved mesh arose from the coarseness of the large CVs at the boundary outside the tunnel, whereby the ambient conditions does not require a sophisticated mesh. Nonetheless, these quality values were all above the recommended quality threshold given by Fluent.

## INITIAL CONDITIONS

Atmospheric pressure i.e. 101325 Pa, and air i.e. 23% $O_2$ and 77% $N_2$ with quiescent conditions, $ui=uj=uk=0$, was set for the entire domain as initial conditions. It is to be noted that for simplification, the part of the gasses with minor concentration, $H_2$, $CH_4$, $CO_2$, were discounted and

given to the concentration of oxygen explaining its higher value originally being 20.1% [22]. To adhere to the notion that the increase of internal pressure in hydrogen prior to ignition due to the tank's engulfment in a bonfire, the near vicinity of the tank was set to envisage only combustion products. The circumference of the patch around the tank had a width double the radius of the tank, and diameter of the tank as the added height of the tank, the patch contains mass fraction 0.1 of $H_2O$ and 0.9 of $N_2$.

The tank was then set to contain only $H_2$ with a pressure of 94.5 MPa and a temperature of 395 K. This was to reflect the conditions of the tank measured right before it catastrophic ruptured in the earlier mentioned experiment [17]. Reproducing the tank rupturing in the simulations was done by setting the tank wall condition as interior, with the volume thereby modelled directly as an instantaneous release of high-pressure hydrogen. The properties of the different size of tanks simulated are listed in Table 2, covering tank sizes currently available for hydrogen-powered vehicles.

**Table 2. Parameters of hydrogen tanks used in rupture simulation in all three different tunnels**

| Volume, L | Real gas tank volume, L | Hemisphere diameter, m | Mass, kg |
|---|---|---|---|
| **10** | 14.5 | 0.25 | 0.58 |
| **30** | 43.1 | 0.45 | 1.73 |
| **60** | 86.0 | 0.61 | 3.45 |
| **120** | 173.5 | 0.77 | 6.96 |

Inside the tunnel, the walls were set to being stationary, impermeable and opaque with diffuse fraction equal to 1 with no-slip conditions omitting any wall roughness. Thermal heat flux was set with a concrete density of 2300 kg/m$^3$, with a wall temperature equal to that of the atmospheric conditions of 280 K. Outside the tunnel, non-reflective properties were applied to ensure any parameter such as energy, mass, momentum etc. not influence the properties inside the tunnel in any way.

## CFL CONVERGENCE

To enforce numerical stability and accurate description of the resolved scales of motion, the time advancement scheme is a meticulous choice to make. The Courant-Friedrichs-Lewy (CFL) number was applied, defined as: $CFL = U\Delta t/\Delta x$, where $\Delta t$ is the time step, $\Delta x$ is the cell size and $U$ is the flow velocity. In compressible flows, the flow velocity is often replaced with the highest velocity of acoustic waves, $|U| + c$ in each cell to make it more applicable. This is useful in terms of limiting the time step, as the isolated convective flow velocity might not be sufficient to capture all the prevailing acoustic wave-speeds. By using a constant CFL number, it in turn reflects not only the time step that would best optimize the solution on a particular grid at particular time step, it also provides an indication of the complexity of a problem, type of flow and model chosen to carry out simulations.

A user defined function (UDF) first developed in house was used to superimpose the CFL number during transient simulations. There was no definite way of predicting the upper bound CFL number, and therefore conducted by trial and error until the convergence is obtained between different CFL numbers. A way of authenticating the applied CFL number is done by conducting a sensitivity test, reducing the value until convergence in the results is found ensuring CFL number independence. As seen in Fig. 4, $CFL \leq 0.2$ was found to give convergence in burned hydrogen, with a corresponding

numerical "loss" in hydrogen mass of close to 0%. Onwards, all simulations were carried out with *CFL* = 0.2.

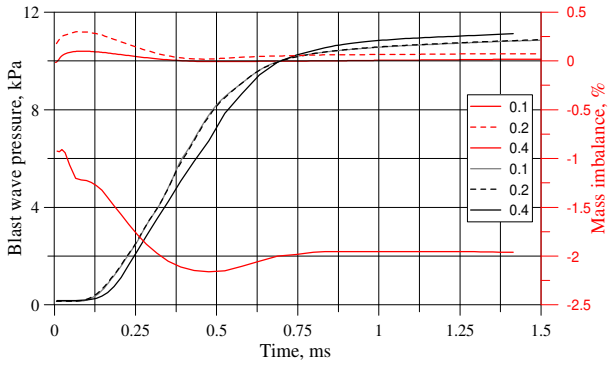


**Fig. 4.** Percentage of hydrogen burned mass (black curves) and imbalance (red curves) for various CFL numbers as a function of time.

## MESH SENSITIVITY

The balance between a fine enough mesh to capture calculations of minor turbulent and diffusive mechanism, but still coarse enough to ensure a practical computational time is always tricky to get just right. The former more crucial, this would ensure that results obtained are not mesh dependent, removing that accuracy-bias from results obtained. A sensitivity test was carried out using two meshes; one coarse with a total control volume number of 176 K, and the other with 486 K denoted as fine mesh. The fine mesh was created by subdividing the cells widths in every direction, which resulted in 8 times (2x2x2) more cells for three-dimensional cells. It is to be noted that the mesh outside the tunnel was kept the same during the mesh sensitivity test. Modelling both meshes gave close convergence in the peak pressure during early stages of simulation when the pressure is most abrupt, with slight under prediction for the coarse grid as can be seen in Fig. 5. The measurements were obtained from 25 cm above the ground where the pressure is maximum, and within 5 CVs which forms the shock front in CFD. Since the case itself is already conservative and things like energy loss on car deformation, cratering, presence of obstacles etc. not taken into account, the coarse grid is therefore utilized in all simulations in order to retain an effective computational time.

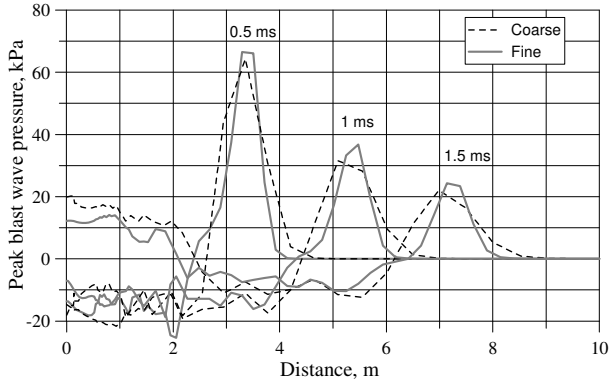


**Fig. 5.** Blast wave pressure along the tunnel for coarse (black dashed) and fine (grey solid) mesh, measured at a height 0.25 m above the ground at 0.5, 1, and 1.5 ms after tank rupture.

## RESULTS AND DISSCUSSION

The results of simulations presented in Fig. 6, where maximum overpressure along the tunnel is plotted as a function of the distance. Also depicted are three horizontal lines representing the three hazard distances thresholds i.e. “no-harm” (green, 1.34 kPa), “injury” (orange, 16.5 kPa) and “fatality” (purple, 100 kPa) [23]. These harm criteria for people thresholds are for each case described as temporal loss of hearing, 1% eardrum rupture probability and 1% fatality probability respectively. The “injury” threshold separates slight and serious injury, such as eardrum rupture and lung haemorrhage as direct effects due to blast wave.

Observed up to 40 m for all tunnels is the dominant oscillating nature of pressure dynamics due to the series of blast reflections. From here onwards, the general trend of all the curves are very similar, the level difference in overpressure originating of the different cross-section areas and mass of hydrogen initially stored in the tank. As this quasi-steady pressure front is established, the pressure attenuation rate is significantly reduced with more than half the pressure retained until the tunnel exit for nearly all cases. In the far field (i.e. after 40 m), all cases of tunnel area and mass combinations fall below the “fatality” zone threshold into the “injury” zone. However, most cases with tank mass above 0.58 kg regardless of the tunnel cross-section are above “injury” threshold during the whole length of the tunnel. The average time blast wave took to reach the exit was 0.45 s.

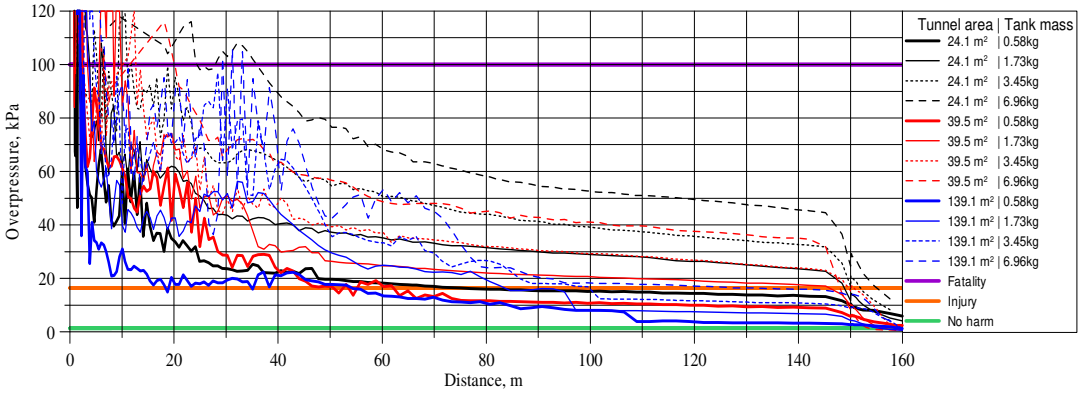


**Fig. 6.** Maximum blast wave pressure as a function of distance from centre of the tank for different tank sizes and tunnel cross-sections.

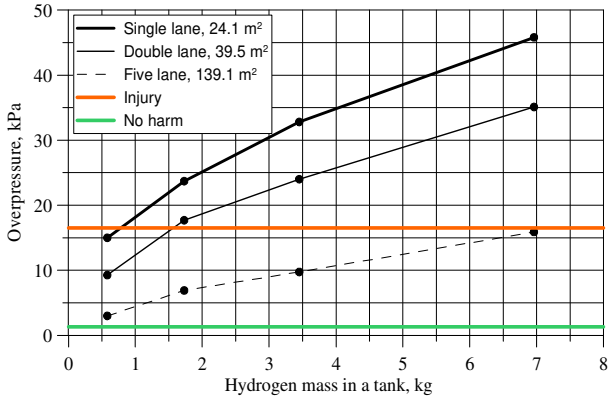


**Fig. 7.** Maximum blast wave pressure recorded at 140 m from the tank as a function of tank mass for three tunnel cross-sections.

Figure 7 shows dependence of the maximum blast overpressure recorded at 140 m i.e. 10 m before the tunnel exit for all three tunnels and various tank inventories. Symbols represent the exact tank inventory for each simulation. Connecting lines give approximate estimation of the overpressure for certain tunnel cross-sections with different amounts of hydrogen inventory. For the singe-lane tunnel hydrogen inventory above 0.75 kg would create overpressure above "injury" limit. For the two-lane tunnel, this minimum inventory mass value is doubled to around 1.6 kg. For the five-lane tunnel, all cases are below the "injury" limit up until 7 kg of hydrogen inventory, the enlarged confinement of the tunnel facilitating a more pronounced pressure decay. The "no-harm" limit is however not obtained at 140 m in any tunnel for hydrogen mass inventories down to 0.58 kg. All cases are well below the "fatality" threshold of 100 kPa.

## CONCLUSIONS

The CFD model for simulation of blast wave and fireball created by high-pressure hydrogen tank rupture in a fire is developed and validated against bonfire test with tank rupture in open atmosphere. The validated model is further applied to simulate blast wave generated in a tunnel, analysing its propagation in such a confined space. Within a 150 m tunnel, results allow graphical estimation of the overpressure at any distance for cross sections ranging between 24-139 $m^2$ and inventory mass of hydrogen from 0.58-6.96 kg at pressure before burst of 94.5 MPa, the worst-case scenario of tank pressure before rupture.

The consequences analysis based on the comparison of harm criteria with pressure generated at distances from the tank rupture along the tunnel has shown that there is no "no-harm" zone. People in the tunnel would encounter fatality in the near field or injury in the far field by the generated blast, an unacceptable consequence. It is worth mentioning that blast damping effects either wise dedicated to propulsion of tank wall and other fragments (i.e. vehicle) are not accounted for in this study.

This is a preliminary study of mainly academic interest rather than a source of safety guidelines for storage tank and hydrogen-powered vehicle developers. However, more research should be done in order exclude injuries and/or fatalities and develop innovative safety technologies to exclude tank rupture in a fire at all. One of such technologies called leak-no-burst is currently under development at Ulster.

## ACKNOWLEDGEMENTS

The authors are grateful to EPSRC for funding through SUPERGEN H2FC Hub (extension) project (EP/P024807/1).

This project has received funding from the Fuel Cells and Hydrogen 2 Joint Undertaking under grant agreement No (736648). This Joint Undertaking receives support from the European Union's Horizon 2020 research and innovation programme, Hydrogen Europe and Hydrogen Europe research.

## REFERENCES

[1] H. T. Hwang, A. Varma, Hydrogen Storage for Fuel Cell Vehicles, Current Opinion Chem. Eng. 5, Suppl. C (2014) 42–48.

[2] S. Kumar *et al.*, HyTunnel Project to Investigate the Use of Hydrogen Vehicles in Road Tunnels, In: International Conference on Hydrogen Safety, 241, Ajaccio, 2009.

[3] M. Dadashzadeh, S. Kashkarov, D. Makarov, V. Molkov, Risk assessment methodology for onboard hydrogen storage, Int. J. Hydrogen Energy 43 (2018) 6462–6475.

[4] A. M. Benselama, M. J.-P. William-Louis, F. Monnoyer, C. Proust, A Numerical Study of the Evolution of the Blast Wave Shape in Tunnels, J. Hazard. Mater. 181 (2010) 609–616.

[5] V. Molkov, F. Verbecke, D. Makarov, LES of Hydrogen-Air Deflagrations in a 78.5 m Tunnel, Combust. Sci. Technol. 180 (2008) 796–808.

[6] S. W. Jorgensen, Hydrogen Storage Tanks for Vehicles: Recent Progress and Current Status, Current Opinion Solid State Mater. Sci. 15(2) (2011) 39–43.

[7] W. J. Taylor, Blast Wave Behavior in Confined Regions, Annals of the New York Academy of Sciences, 152 (1968) 339–356.

[8] B. W. Skews and W. R. Law, The Propagation of Shock Waves in a Complex Tunnel System, J. of South Africa Inst. Min. Metallurgy 91(4) (1991) 137–144.

[9] D. Uystepruyst and F. Monnoyer, A Numerical Study of the Evolution of the Blast Wave Shape in Rectangular Tunnels, J. Loss Prevent. Process Ind. 34 Suppl. C (2015) 225–231.

[10] W. E. Baker, P. A. Cox, P. S. Westine, J. J. Kulesz, and R. A. Strehlow, Explosion Hazards and Evaluation, Elsevier Scientific Publishing Company, 1983.

[11] R. Zalosh , N. Weyandt, Hydrogen Fuel Tank Fire Exposure Burst Test, SAE Paper, vol. 2005-01–1886, (2005).

[12] W. Kim, V. Shentsov, D. Makarov, V. Molkov, High Pressure Hydrogen Tank Rupture: Blast Wave and Fireball, Intentional Conference on Hydrogen Safety, Yokohama, Japan, 2015, Vol. 243.

[13] N. Weyandt, Analysis of Induced Catastrophic Failure of a 5000 psig Type IV Hydrogen Cylinder, Southwest Research Institute Report for the Motor Vehicle Fire Research Institute, 01.06939.01.001, 2005.

[14] V. Molkov and S. Kashkarov, Blast Wave From a High-Pressure Gas Tank Rupture in a Fire: Stand-Alone and Under-Vehicle Hydrogen Tanks, Int. J. Hydrogen Energy 40 (2015) 12581–12603.

[15] V. Shentsov, D. Makarov, and V. Molkov, Blast Wave After Hydrogen Storage Tank Rupture in a Tunnel Fire, International Symposium on Tunnel Safety and Security 2018, Borås, Sweden, 2018.

[16] S. Mannan, Lees' Loss Prevention in the Process Industries, 3rd ed., vol. 1. Elsevier Butterworth-Heinemann, 2005.

[17] Y. Tamura, M. Takahashi, Y. Maeda, H. Mitsuishi, J. Suzuki, S. Watanabe, Fire Exposure Burst Test of 70MPa Automobile High-pressure Hydrogen Cylinders, Society of Automotive Engineers of Japan Annual Autum Congress, 2006.

[18] B. Maidl, M. Thewes, U. Maidl, General Principles for the Design of the Cross-Section, Handbook of Tunnel Engineering *II*, D-69451 Weinheim, Germany: Wiley-VCH Verlag GmbH, pp. 1–20, 2014.

[19] M. Vickers, Northern California Coastal Bridges: Picturesque and Distinctive Spans, Marquis Publishing, 2017.

[20] W. Brilon and F. Weiser, Two-Lane Rural Highways: The German Experience, Transportation Research Record, J. Transport. Res. Board, 1988, (2006) 38–47.

[21] Norwegian Public Roads Administration, Road Tunnels, Statens vegvesen, 21, 2004.

[22] ANSYS FLUENT 12.0 User's Guide, Available: http://users.ugent.be/~mvbelleg/flug-12-0.pdf, 2009 (accessed: 30 September 2018).

[23] S. Kashkarov, Z. Y. Li, V. Molkov, Hazard Distance Nomograms for a Blast Wave From a Compressed Hydrogen Tank Rupture in a Fire, International Conference on Hydrogen Safety, Hamburg, 2017, Vol. 126.